Accelerated mineral carbonation of stainless steel slags for CO_2 storage and waste valorization: effect of process parameters on geochemical properties

Rafael M. Santos [a,*], Jens Van Bouwel [a], Ellen Vandevelde [a], Gilles Mertens [b,1], Jan Elsen [b], Tom Van Gerven [a]

[a] Department of Chemical Engineering, KU Leuven, Willem de Croylaan 46, 3001 Leuven, Belgium

[b] Department of Earth and Environmental Sciences, KU Leuven, Celestijnenlaan 200e, 3001 Leuven, Belgium

[1] Present address: Qmineral bvba, Romeinsestraat 18, 3001 Heverlee (Leuven), Belgium.

* Corresponding author. Tel.: +32 16 322350; fax: +32 16 322991.

E-mail addresses: rafael.santos@cit.kuleuven.be (R.M. Santos); tom.vangerven@cit.kuleuven.be (T. Van Gerven).

ABSTRACT

This work explores the mineral carbonation of stainless steel slags in search for a technically and economically feasible treatment solution that steers these waste residues away from costly disposal in landfills and into valuable applications. Argon Oxygen Decarburization (AOD) and Continuous Casting (CC) slags prove ideal for mineral carbonation as their powdery morphology forgoes the need for milling and provides sufficient surface area for high reactivity towards direct aqueous carbonation. Experiments were undertaken using two methodologies: unpressurized thin-film carbonation, and pressurized

DOI:10.1016/j.ijggc.2013.04.004

slurry carbonation. The influence of process parameters (temperature, CO_2 partial pressure, time, solids loading) on the slag carbonation conversion are investigated, seeking the optimal conditions that maximize the potential of the slags as carbon sinks. It was found that CC slag carbonates more extensively than AOD slag at essentially every processing condition due to differences in particle microstructure; still, it was possible to reach up to 0.26 and 0.31 g,CO_2/g,slag uptake with AOD and CC slags, respectively, at optimal processing conditions via pressurized slurry carbonation. Mineral carbonation conversion was accompanied by significant reduction in basicity, as much as two pH units, and stabilization of heavy metals leaching, meeting regulatory limits (borderline for Cr) for safe waste materials re-use. Via quantitative mineralogical analyses, it was possible to differentiate the carbonation reactivity of several alkaline mineral phases, and to discern the preferential formation of certain Ca- and Mg-carbonates depending on the processing route and operating conditions. Slurry carbonation was found to deliver greater mineral carbonation conversion and optimal treatment homogeneity, which are required for commercial applications. However, thin-film carbonation may be a more feasible route for the utilization of slags solely as carbon sinks, particularly due to the elimination of several processing steps and reduction of energy demand.

Keywords: mineral carbonation; stainless steel slags; carbon sink; waste valorization; mineralogy; heavy metal leaching.

1. Introduction

Mineral carbonation involves the capture of carbon dioxide in a mineral form by its reaction with alkaline materials, composed of calcium- and magnesium-rich oxides and silicates, leading to the formation of solid carbonate products (Lackner et al., 1997). The principal aim and advantage of this approach is the geochemical stability and storage safety of mineral carbonates, the opportunities for process integration presented by the technology, due to the exothermicity of the reaction, that enable energy efficiency gains, and the potential for valorisation of otherwise low-value resources (virgin or waste) into useful products. However, several barriers still limit the deployment of mineral carbonation in industry, which, apart from the lack of legislative mandates for carbon capture and a sustainable CO_2 pricing scheme, include: the high energy intensity, slow reaction kinetics and low reaction conversions of traditional processing routes; complexities of the production chain and process

adaptability; and competition for attention with alternative carbon capture technologies (such as geological carbon capture and storage (CCS)). Matching the right alkaline materials with the right mineral carbonation processes is key to overcoming the barriers that prevent this technology from reaching the market (Santos and Van Gerven, 2011).

Steel slags, by-products of steel production processes, are a widely available class of industrial waste materials that can potentially benefit from mineral carbonation through the reduction in basicity (pH), swelling stabilization, and reduction of heavy metals leaching (Baciocchi et al., 2010; Huijgen and Comans, 2006; Santos et al., 2012b, 2012c). Moreover, their high CO_2 uptake capacities, coupled to the large on-site CO_2 emissions of steelworks, offers opportunities for carbon capture credit gains. To date, most research on single-step aqueous carbonation of steel slags have focussed on Basic Oxygen Furnace (BOF) slag, originating from the second processing step of carbon steel production and notably studied by Huijgen et al. (2005) Huijgen and Comans (2006) and Chang et al. (2011a, 2011b, 2012, 2013), and Electric Arc Furnace (EAF) slag, originating from the first step of the stainless steel production, with results recently reported by Baciocchi et al. (2010, 2011). However, a main disadvantage to the carbonation of these residues is the milling requirement to generate sufficient reactive surface area, as these slags solidify upon cooling in the form of monoliths.

The present study focuses instead on two additional slags produced from the stainless steel process that possess powdery morphology and can benefit in a more energy efficient manner from mineral carbonation: Argon Oxygen Decarburization (AOD) slag, and Continuous Casting (CC) slag, also referred to as Ladle Metallurgy (LM) slag. These fine powders cause severe dusting issues during handling and storage in the steelworks; furthermore, the slag in this form cannot be readily re-utilized or valorised, and often must to be landfilled (Domínguez et al., 2010). Concerns regarding drainage from steel slag disposal sites, which can be extremely alkaline and a source of pollution to surface and ground waters (Mayes et al., 2008), add to the disposal costs. Treatment strategies including the addition of stabilizing ions, silica and rapid cooling, which aim at preventing the disintegration of the slags by hindering the expansive β- to γ- transformation of dicalcium silicate (C2S), have been tested and, in some cases, implemented in industry (Durinck et al., 2008). However costly and energy intensive processes, hazardous additives (boron), and low-value final products still force the industry to search for more sustainable solutions.

Prior to the present study, we have reported in Santos et al. (2012b) findings on the carbonation of AOD and CC slags under atmospheric pressure bubbling slurry conditions, with and without the use of ultrasound for intensification of the reaction. Therein it was found

that at 50 °C and for up to 4 h reaction time, sonication increased the reaction rate, achieving higher carbonation conversion and lower basicity. AOD slag Ca-conversion increased from 30% to 49%, and pH decreased from 10.6 to 10.1, while CC slag Ca-conversion increased from 61% to 73% and pH decreased from 10.8 to 9.9. The enhancement effect of ultrasound was attributed to the removal of passivating layers (precipitated calcium carbonate and depleted silica) that surround the unreacted particle core and inhibit mass transfer. However, an efficiency analysis pointed to significant challenges for scale-up of this technology, due to the high energy consumption of the ultrasound process, resulting in net negative CO_2 capture.

In search of more feasible processing conditions (technically and sustainably), this work explores two additional routes for the mineral carbonation of AOD and CC slags: (i) unpressurized thin-film carbonation, and (ii) pressurized slurry carbonation. Both methodologies are viewed as offering lower energy intensity compared to ultrasound carbonation, the former being performed under passive/mild conditions, while the latter has the potential to deliver reaction rate intensification in a more efficient manner. Herein, experiments are undertaken to investigate the influence of process parameters (temperature, CO_2 partial pressure, time, solids loading) on the slag carbonation kinetics, including CO_2 uptake and mineral conversion, seeking the optimal conditions that maximize the potential of the slags as carbon sinks. The heavy metal leaching and basicity behaviours are also evaluated to characterize the geochemical character of the carbonated materials, whose mineralogical composition, including the formed carbonate phases, are assessed and quantified.

2. Materials and methods

2.1 Materials characterization methodologies

The chemical composition of the slags was determined by X-ray Fluorescence (XRF) analysis, using a sequential wavelength dispersive spectrometer (PANalytical PW 2400) and SuperQ software for quantification; measurement uncertainty is approximately ± 2 units of the last significant figure reported, and verifiable detection limit is ~0.01 wt%. The volume-based particle size distributions and the average particle diameters, expressed as D[4,3] (volume moment mean diameter) and D[3,2] (surface area moment mean diameter) were determined by wet Laser Diffraction (LD, Malvern Mastersizer) in sonicated deionized water, with a measurement uncertainty of ± 5 %, determined by replicates, and detection range of

0.06–878.7 μm. The morphology of fresh and carbonated powders was observed by Scanning Electron Microscopy (SEM, Philips XL30) and inspected with Energy-dispersive X-ray Spectroscopy (EDX).

The mineralogical composition of the slags was determined by semi-quantitative X-Ray Diffraction (QXRD), adapting the methodology of Snellings et al. (2010). Measurements were performed on a Philips PW1830 equipped with a graphite monochromator and a gas proportional detector, using Cu Kα radiation at 30 mA and 45 kV, step size of 0.03° 2θ and counting time of 2 s per step, over 10–65° 2θ range. Mineral identification was done in Diffrac-Plus EVA (Bruker) and mineral quantification was performed by Rietveld refinement technique using Topas Academic v4.1 (Coelho Software). Mahieux et al. (2010) verified that QXRD of complex mineral wastes can be performed coherently and reliably, though it inherently carries a level of uncertainty. In this work the 'goodness of fit', calculated in Topas, for AOD and CC slag samples averaged to 1.45 ± 0.09 and 1.42 ± 0.13, respectively. Mineral composition and conversion values were calculated based on the methodology detailed in our recent study reported in Bodor et al. (2013), whereby the mass fractions delivered by Rietveld analysis are translated into molar fractions normalized against the pre-carbonation mass of the materials (to discount the CO_2 uptake mass after carbonation, which artificially lowers the mass fractions of non-carbonate components) and the formation of amorphous materials during carbonation is taken into account (which, if ignored, causes overestimation of mineral mass fractions) by utilizing the calcium mass balance as a reference. This data handling procedure enhances the accuracy of conversion values and allows for more precise comparison of the results, as opposed to the simple comparison of pre-carbonation composition to post-carbonation composition. Mean quantification accuracy, based on replicate analyses, has been estimated for steel slags in the present study at ± 2.3 wt% of the quantified amount.

The CO_2 uptake of carbonated materials was quantified by Thermal Gravimetric Analysis (TGA, Netzsch STA 409). An amount of ~100 mg sample was weighed in a sample pan heated from 25 to 900 °C under nitrogen flow at a heating rate of 15 °C/min. The weight loss was recorded by the TGA microbalance and the amount of CO_2 released was quantified by the weight loss between 300–800 °C. It was verified using pure Ca- and Mg-carbonates (Fig. S1 in the Supplementary Content) that this temperature range covers the CO_2 release region, and excludes the low temperature region where hydrates decompose. While this temperature range also overlaps with the dehydroxylation region of $Ca(OH)_2$ (~340–430 °C), the interference is assumed to be negligible due to the lack of evidence of the formation of

hydroxylated products by XRD and Fourier transform-infrared (FTIR). The method reproducibility, caused by sample size and inhomogeneity, and assessed by replicates, was ± 2 %. Carbonation conversion is then calculated as the ratio of CO_2 uptake experimentally determined to the theoretical CO_2 uptake capacity of the slag (given in section 2.2). Loss on ignition (LOI) of fresh samples was also determined by TGA, and quantified by the weight loss between 25 and 800 °C. FTIR spectra of sample powders were recorded on a Perkin Elmer Frontier spectrometer with attenuated total reflection (ATR) accessory in the region of 4000–650 cm^{-1} at a resolution of 1 cm^{-1}.

Determination of aqueous elemental concentrations was performed by Inductively Coupled Plasma Mass Spectroscopy (ICP-MS, Thermo Electron X Series); measurement accuracy, determined using standard solutions (diluted from 1000 mg/L Merck CertiPUR elemental standards), was ± 2 %.

2.2 Stainless steel slags

The AOD and CC stainless steel slags were obtained from a Belgian steelworks. The materials were freshly collected from the production process, and were stored in sealed containers to avoid atmospheric weathering. It was verified by TGA that the CO_2 contents of the uncarbonated slags at the completion of the study were < 0.010 g,CO_2/g,slag. Prior to analyses or experimentation, the materials were sieved to < 500 µm particle size to remove a small portion of coarse particles (< 5 wt%). Particle size distributions, determined by LD, are presented in Fig. S2 in the Supplementary Content, and indicate bimodal distributions with maxima between 0.1–1 µm and 10–100 µm. AOD slag has D[4,3] = 46.1 µm and D[3,2] = 3.9 µm, and CC slag has D[4,3] = 39.3 µm and D [3,2] = 2.8 µm.

The chemical compositions of the slags, determined by XRF analysis, are presented in Table 1. Both slags contain high concentrations of calcium and moderate concentrations of magnesium, components which imparts these materials their alkaline properties and reactivity towards mineral carbonation. These values are used for calculating the maximum theoretical CO_2 uptake capacities of the slags. AOD and CC slags have CO_2 uptake capacity of 0.528 and 0.520 g,CO_2/g,slag, respectively. Expressed as mass percentages, these values correspond to 34.2 and 34.6 wt%,CO_2, respectively. Trace elements detected by XRF, present in quantities of 0.1–0.01 wt%, are, in decreasing order: AOD: Sr, Nb, V, La, Cl, Zr; CC: V, K, Cl, Nb, Ni, Sr, Zn, Mo, Pb.

The mineralogical compositions of the slags, determined by QXRD, are presented in Table 2. The diffractograms of these materials are provided in Fig. S3 in the Supplementary Content. The main mineral phase of both AOD and CC slags is gamma-dicalcium-silicate (γ-C2S, Ca_2SiO_4), of which the latter contains significantly greater amount. AOD slag notably contains greater quantities of bredigite ($Ca_{14}Mg_2(SiO_4)_8$), cuspidine ($Ca_4Si_2O_7F_2$), β-C2S (Ca_2SiO_4), and merwinite ($Ca_3Mg(SiO_4)_2$), while CC slag possesses significantly more periclase (MgO) and enstatite ($Mg_2Si_2O_6$).

2.3 Thin-film carbonation methodology

Thin-film carbonation consists in reacting moist solids with a CO_2/air mixture within an incubator. The slag samples were initially wetted with ultrapure water to obtain 25 wt% moisture content: 100 g mixed with 33.3 ml H_2O. This moisture content was determined as optimal based on preliminary tests performed by Vandevelde (2010) and reported in Santos et al. (2010). These studies showed that it is necessary to maintain the moisture content between 10–35 wt% for the duration of the experiment to sustain the thin-film carbonation reaction, which was aided by maintaining near saturation relative humidity. This serves to minimize sample dry-out that can occur due to the exothermic heat of reaction during carbonation, and to prevent flooding of the sample, which can hinder the diffusion of CO_2 towards the reaction front at the solid-liquid interface. Also reported were superior carbonation performances at 30 °C (versus 50 °C) and at 20 vol% CO_2 partial pressure at 1 atm total pressure (versus 10 vol%), as a result of improved CO_2 solubility under these conditions.

In the present study, the moist pastes were thinly spread on trays and placed in a CO_2–chamber (Sanyo CO_2 incubator MCO-17, pictured in Fig. S4 in the Supplementary Content) at 30 °C, under a CO_2 partial pressure of 0.2 atm (balance air) and ~95% relative humidity. The samples were rewetted during the experiment, at 26 h (addition of 13.3 ml H_2O, or 2/5 of initial moisture content) and at 94 h (addition of 20 ml H_2O, or 3/5 of initial moisture content). At the same time as re-wetting, samples were lightly deagglomerated using a pestle, as carbonation can lead to cementitious behaviour of the stationary material, thus decreasing powder surface area and hindering carbonation progression (Vandevelde, 2010). Intermediate samples were collected at these times and dried at 60 °C for 24 h. The remaining carbonated samples were removed from the CO_2–chamber after six days (144 h) of carbonation, and subsequently dried at 60 °C for 24 h. The weight change during drying was used to determine free moisture content of the collected samples.

DOI:10.1016/j.ijggc.2013.04.004

2.4 Slurry carbonation methodology

Slurry carbonation of stainless steel slags was conducted in a Büchi Ecoclave 300 Type 3E autoclave reactor (Büchi Glas Uster AG, pictured in Fig. S5 in the Supplementary Content) of 1.1 litre internal volume, equipped with cyclone impeller stirrer (0 to 2000 rpm), electric-heating/water-cooling jacket, and capable of operating at pressures of 0 to 60 bar_g and temperatures of 20 to 250 ^oC. Experiments were conducted using 800 ml ultrapure water, 1000 rpm stirring speed and industrial grade (99.5 % purity) CO_2 (Praxair). Process parameters varied were: temperature (*T*, 30–180 °C), CO_2 partial pressure (*P*, 2–30 bar), reaction time (*t*, 5–120 min), and solids loading (*S*, 25–250 g/L). Parameters were varied individually, using the following median condition as a baseline: 90 °C, 6 bar,CO_2, 60 min, and 62.5 g/L. The carbonated slurry was vacuum filtered using Whatman 5 filter paper (2.5 μm nomimal pore size) and the recovered solids were oven dried at 105 °C for 4 h. Select experiments were performed in duplicate for data validation; average reproducibility of measured carbonation conversion, determined in similar manner as Huijgen and Comans (2006), was ± 2.9 % (reproducibility data presented in Fig. S6 in the Supplementary Content). Geochemical modelling of aqueous carbonation equilibria was performed using Visual MINTEQ (ver. 3.0, KTH). The activity coefficients were calculated using the Davies equation, valid for the ionic strengths modelled here (< 1 M), and the gas solubilities were found to be in good agreement with the experimental and modeling data presented in Rosenqvist et al. (2012).

2.5 Batch leaching test methodology

Leaching tests were performed, in triplicates, on fresh and carbonated slag samples to determine the effect of carbonation on the mobility of regulated metals and on the material basicity. For each sample, an amount of 10 grams of solids was mixed with 100 ml ultrapure (18.2 MΩ·cm) water (*L/S* = 10) in a sealed PE bottle, and shaken on a vibration table (Gerhardt Laboshake) at 160 rpm and 25 °C for 24 hours. Solution pH was measured to determine basicity (± 0.1 pH units); basicity values were compared to the values of pure carbonates modelled using Visual MINTEQ. The leaching solution was filtered with 0.45 μm membrane filter prior to dilution for ICP-MS measurement; solution matrix was 0.3 M nitric acid. Elemental concentration reproducibility, based on replicates, averaged ± 15 %. Table 3

presents heavy metals and metalloids detected and their respective leaching limits (in milligrams metal leached per kilogram dry solid) according to Belgian Walloon regulations for secondary materials re-use in non-structural applications (Ministère de la Région Wallonne, 2001).

3. Results

3.1 CO_2 uptake

3.1.1 Thin-film carbonation CO_2 uptake

Thin-film carbonation experiments were conducted to assess the carbonation extent and the geochemical changes resulting from mineral exposure to CO_2 at mild operating conditions, in view of developing a technically and economically feasible process for industrial implementation of stainless steel slag carbonation. Results of the thin-film carbonation experiments on AOD and CC slags are presented in Fig. 1 in the form of thermogravimetrical curves. The mass loss upon heating is directly correlated to the decomposition of carbonates and hydrates, which occur at discrete temperature ranges, and thus can be used to estimate carbonation conversion as the ratio between actual CO_2 uptake and theoretical CO_2 uptake capacity.

Two distinct mass loss regions are observed, one below 250 °C, and another between 600–800 °C. The former can be attributed to loss of H_2O from chemically bonded water, while the latter belongs to the $CaCO_3$ decomposition reaction. Between 250–600 °C the curves display gradually declining slopes. This temperature range corresponds to a number of possible reactions, including dehydroxylation and magnesium-containing carbonate decompositions reactions, such as those indicated in Fig. S1 and reported by Hollingbery and Hull (2012), and the decomposition of amorphous or poorly crystalline carbonate species, reported by Cizer et al. (2012). In any case, the mass losses in this intermediary temperature range are significantly smaller than at the comparatively high and low temperature ranges, meaning that small quantities of these species are formed.

It is observed by inspection of the trends in Fig. 1 that the reaction extent of CC slag is greater than that of AOD after 94 hours for all three temperature ranges, indicative of greater formation of all aforementioned species. This is quantified by the carbonation conversion values presented, where CC slag achieves 28.0 % conversion at 94 hours, compared to

19.0 % for AOD slag, and 37.0 % conversion after 144 hours, compared to 24.2 % for AOD slag. During the first 26 hours, however, the carbonation extents of both slags are comparable. This suggests that carbonation kinetics of both slags are initially similar, just as their chemical and mineralogical compositions are also similar, but the progression of AOD slag carbonation becomes hindered earlier than in the case of CC slag.

Passivating layers composed of carbonate products, residual silica and unreactive minerals were shown in our previous study (Santos et al., 2012b) to form during mineral carbonation, restricting contact between the unreacted core and the dissolved CO_2 in the aqueous medium and thus slowing down or even stopping the reaction progress. In that study, performed using atmospheric pressure bubbling slurry conditions, carbonation conversion values (recalculated to account for the sum of Ca and Mg content of the slags) for AOD and CC slags reached plateaus at 25.8 % and 48.5 %, respectively, after four hours of reaction time (and without using sonication for removal of passivating layers). The results in the present study, though reached only after extensively longer processing times, are comparable, suggesting that the reaction extent limitation mechanism may be similar. Additional thin-film carbonation processing time may still marginally increase conversion under the tested conditions, but this would be unattractive from an industrial application perspective.

In the present thin-film carbonation methodology, two additional factors can play a role in limiting reaction progression: (i) sample moisture, and (ii) cementitious behavior of the sample paste. The exothermic heat of the carbonation reactions partially evaporates water from the sample paste over time. Water can also be consumed in the carbonation reactions through the formation of hydrated mineral phases (e.g. calcium-silicate-hydrate (CSH), monohydrocalcite ($CaCO_3 \cdot H_2O$), hydromagnesite ($Mg_5(CO_3)_4(OH)_2 \cdot 4H_2O$), nesquehonite ($MgCO_3 \cdot 3H_2O$), etc.). Insufficient moisture can significantly reduce or even cease the rate of reaction (Vandevelde, 2010). Table 4 presents the moisture content of the slags as a function of time. The moisture content of CC slag drops significantly more than that of AOD slag. Between the 3 and 26 hour samplings, the moisture content of CC slag is reduced by 9.1 wt%, versus 4.3 wt% for AOD slag. At the 94 hour sampling, despite prior re-wetting, CC slag moisture is only 3.8 wt%, while AOD moisture is stabilized near 18 wt%. At the 144 hour sampling the moisture content of CC slag is again much lower than that of AOD slag, despite prior re-wetting at the 94 hour mark. Lowering of CC slag moisture content, however, does not appear to significantly hinder reactivity towards carbonation, as it achieves greater carbonation extent than AOD slag (as previously shown in Fig. 1). In fact, the moisture loss

can be proportionally related to carbonation conversion, as well as to the formation of hydrated phases suggested by the mass loss measured by TGA at temperatures below 250 °C.

In terms of cementitious behavior, both slags presented hardening during carbonation. This phenomenon is caused by aggregation of precipitating carbonate crystals that bond individual particles and form a solid matrix. This behavior has led to the investigation of using stainless steel slags as binders in construction materials applications (Kriskova et al., 2012). However, for carbonation purposes, this behavior can potentially lead to reduced paste porosity and permeability, and thus hinder carbonation progression. Comparatively, as assessed during deagglomeration of the material by mortar and pestle during re-wetting, CC slag hardened more and continued to harden after each sampling, while AOD slag hardening decreased as a function of time. Therefore, it does not appear that the cementitious behavior is the principle reason for the inferior carbonation performance of AOD slag. Cizer et al. (2012) propose that the evaporation of water decreases the pore water content and allows better diffusion of gaseous CO_2 into the bulk volume of lime paste through the open paths formed along the sample depth, thus aiding carbonation progression. Additional possibilities for lower AOD slag reactivity are particle morphology and microstructure, and its mineralogical composition, which are assessed in section 3.2.

3.1.2 Slurry carbonation CO_2 uptake

Slurry carbonation experiments were conducted to assess the carbonation extent and the geochemical changes resulting from mineral exposure to CO_2 at a range of process conditions, seeking to intensify the mineral carbonation reaction and thus achieve greater CO_2 uptake and carbonation conversion than previously tested methods. Slurry carbonation also has the benefit, versus thin-film carbonation, of improved mass transfer and enhanced particle attrition, due to continuous mixing of the solids in suspension. Fig. 2 shows the results of the slurry carbonation experiments on AOD and CC slags, where the effect of four process variables (T, $P(CO_2)$, t, and S) on the carbonation conversion (expressed as percentage of the maximal CO_2 uptake), determined by TGA, is presented.

Under nearly all conditions tested, CC slag carbonation conversion surpassed that of AOD slag when exposed to identical process parameters, in agreement with previously tested methodologies. This reaffirms that slag mineralogy, morphology and microstructure are the likely causes for this discrepancy; more details on this investigation in section 3.2. The effect of temperature on carbonation conversion of both slags appears to be small (Fig. 2a).

However, it should be noted that experiments with temperatures above 100 °C required additional cooling time prior to depressurization, up to 60 minutes in the case of 180 °C. Since CO_2 remained present in the reactor during cooling, carbonation reaction likely continued over time, and also at different temperatures until reaching 100 °C, when the reactor was opened. This may explain why the negative effect of high temperatures, namely reducing CO_2 solubility (depicted in Fig. 3), is not seen. Still, in the case of CC slag, carbonation conversion did not surpass those achieved at 90 °C and below, while in the case of AOD, slight improvement is seen, particularly comparing results at 90 °C and 120 °C. As the cooling time at 120 °C was only in the order of five minutes, the moderately higher temperature appears to have contributed to its carbonation conversion, though no further benefit is seen from higher temperature experiments. It should also be noted that this series of experiments was conducted using 6 bar,CO_2; the influence of temperature under different baseline partial pressures may differ. For instance, at lower pressures the CO_2 solubility is more significantly affected by temperature than at higher pressures (Fig. 3).

The CO_2 partial pressure resulted in more significant changes in carbonation conversion (Fig. 2b). Up to 9 bar, both slags responded well to increased pressure, displaying conversion improvements in the order of 15 %. After this point, CC slag displayed a peculiar reduction in conversion in the order of 20 %, which only recovered to previous levels at 20 bar; this trend was absent from AOD slag results. As such, maximal CC slag conversion occurred both at 9 and 30 bar, while AOD slag conversion peaked at 15 bar. Mechanistically, increased CO_2 pressure results in greater CO_2 solubility, but also in lower solution pH (Fig. 3), due to the formation and dissociation of carbonic acid. The complex equilibria result in increased $CaCO_3$ solubility at higher pressure, but even at 30 bar and 30 °C total dissolved Ca remains below 1.5 g/L (Fig. 3). This explains why increased pressure is not detrimental to carbonation conversion.

Prolonged reaction time proportionally increased carbonation conversion of both slags (Fig. 2c). Carbonation reactivity was found to be very fast; within one minute of carbonation time carbonation conversion of AOD and CC slags reached 17.1 % and 23.3 %, respectively. Thereafter carbonation conversion continued to increase in approximately linear fashion up to 120 minutes. During the first 30 minutes the conversion difference between AOD and CC slags remained around 7 %, and widened to 12 % after 120 minutes. The slopes of the curves suggest that additional reaction time may further increase conversion, but that they would unlikely surpass roughly 50 and 60 % for AOD and CC slags, respectively. The values at 120 minutes, however, are similar to maximal conversion obtained in our previous study (Santos

et al., 2012b) when using sonication. Hence the increased temperature, pressure and better mixing of the present study serve as efficient alternatives for the intensification of the mineral carbonation reaction compared to the energy intensive sonication applied at milder process conditions. On the other hand, sonication of the slurry at present intensified conditions could serve to speed reaction conversion, particularly after the 15 minute mark when diffusion through the passivating layers, pictured in Fig. 4, becomes rate limiting.

The last parameter changed during slurry carbonation was solids loading (Fig. 2d). It is not expected that solids loading should have a significant effect on carbonation conversion due to exhaustion of dissolved CO_2, especially at prolonged reaction times. Rather, solids loading can affect the rate and intensity of interparticle collisions, and the mixing efficiency. CC slag results suggest that diminished particle interaction, and consequently surface erosion, limits carbonation conversion. This effect, however, is not seen in the case of AOD slag. At high solids loading both slags exhibit a drop-off in carbonation conversion, which can be due to poorer mixing of the dense slurry, and consequently lower mass transfer rates as well as reduced particle collisions. This effect is also greater in the case of CC slag. The mild effect of solids loading on carbonation conversion bodes well for scale-up of this technology, as industrial implementation can benefit from the decreased reactor volume required for the treatment of dense slurries. Furthermore, better mixer, reactor geometry and baffle configuration designs can likely extend the carbonation conversion drop-off to higher solids loadings. To conclude, it can be said that the maximum achievable CO_2 uptake capacities of AOD and CC slags, assuming 50 % and 60 % maximal conversions, are 0.264 and 0.312 g,CO_2/g,slag (or 20.9 and 23.8 wt%), respectively.

3.2 Mineralogy

Stainless steel slags consist of a mixture of mineral phases, including several varieties of alkaline silicates (e.g. bredigite, cuspidine, β- and γ-dicalcium silicates (C_2S), and merwinite) and (hydr)oxides (e.g. brucite, lime, periclase and portlandite). It is likely that these different minerals have different carbonation affinities and kinetics. Doucet (2010) showed that even in 0.5 M HNO_3, only 70–90% of Ca and 40–80% of Mg are leached from finely milled BOF and EAF slags. Moreover, different phases may respond differently to changes in mineral carbonation process conditions (i.e. temperature and pressure). Such behaviors may help explain why the maximal achievable carbonation conversions presented in the previous section are significantly lower than the theoretical capacities.

Additionally, the morphological configuration of the mineral phases can affect the exposure of different minerals to the reacting aqueous medium. Fig. 4 suggests that individual particles of fresh CC slag are primarily composed of specific minerals, as they display clear morphological differences (more images provided in Fig. S7 in the Supplementary Content). Inspection of individual particles by EDX (presented in Fig. S8 in the Supplementary Content) demonstrated that rod shaped particles consist of calcium silicate (recent studies by our group on pure synthetic minerals, reported in Bodor et al. (2013), confirmed such crystalline morphology belonging to γ-C_2S). The chemical composition of particles of apparent smooth surface corresponded well to periclase, while two chemistries of coarse particles were observed, correlating well with β-C_2S and calcium-magnesium silicates. AOD slag particles do not possess discernible morphological features, and EDX analysis did not distinguish particular mineral chemistries. It thus appears that the crystallization of these two slags upon cooling differs, either due to slight differences in chemical composition or due to differences in the cooling paths they undergo in the production process (e.g. quenching rates).

Carbonated slag samples were analyzed by QXRD to elucidate the behavior of the major alkaline mineral phases towards mineral carbonation. Time-dependent results of thin-film and slurry carbonation samples are presented in Figs. 5 and 6, respectively. Pressure- and temperature-dependent results of slurry carbonation samples can be found, respectively, in Figs. S9 and S10 in the Supplementary Content. Despite using the QXRD data handling procedure of Bodor et al. (2013) to enhance the accuracy of conversion values and allows for more precise comparison of the results, as opposed to the simple comparison of pre-carbonation composition to post-carbonation composition, the semi-quantitative nature of the Rietveld analysis of complex mineral samples is reflected in the magnitude of the error bars, which are intuitively larger for phases present in smaller quantities in the slags.

It is observed in Fig. 5 that the carbonation conversion of C2S polymorphs dominates the CO_2 uptake of both slags during thin-film carbonation. Bredigite conversion also reaches significant values, contributing well to AOD slag CO_2 uptake given its large content. Cuspidine, merwinite and periclase reactivities are comparatively poor in both slags; some low extent observed conversions of these minerals may be due to quantification variability caused by diffraction peak overlap, reducing confidence in these trends. It appears that the better carbonation conversion of γ-C2S in CC slag over AOD slag, and the greater content of this mineral phase in CC slag over AOD slag, largely accounts for the higher CO_2 uptake achieved by CC slag over prolonged thin-film carbonation reaction times.

Mineral conversion is generally significantly improved in slurry carbonation, as observed in Fig. 6. Partial carbonation conversion is observed for nearly all reported phases in both slags. The conversion of β-C2S and γ-C2S appears to occur and stabilize faster, while the carbonation conversions of bredigite, cuspidine and periclase generally improve over time. The latter two phases were poorly reactive in thin-film carbonation; hence benefit most from the increased intensity of slurry carbonation. Merwinite appears to react well in CC slag, but remained essentially unconverted in AOD slag; though uncertainty in the CC slag composition value (7 wt%) could contribute to overestimation of its conversion in this slag. It is otherwise difficult to identify mineralogical reasons for the better CO_2 uptake of CC slag over AOD slag, as quantification uncertainties can mask the differences of concurrently converting minerals.

Mineral conversion values as a function of temperature (see Fig. S9) did not display particularly conclusive trends, with the exception of improved γ-C2S carbonation from AOD slag at higher temperatures. As the overall CO_2 uptake values of these samples were quite similar (as previously presented in Fig. 2a), it can be said that temperature does not appear to promote the reactivity of any particular phase (at 6 bar CO_2 partial pressure). Carbonation pressure had a more noticeable effect on AOD slag mineralogy (see Fig. S10), with meaningful improvements in β-C2S, merwinite and periclase conversions at higher pressures. The noticeably lower CO_2 uptakes of CC slag at 12-15 bar (Fig. 2b), however, appear to be related to decreased reactivity of these same mineral phases under these intermediary conditions.

It was also possible to utilize QXRD analysis to assess the formation of different carbonate mineral phases. Time-dependent results of thin-film and slurry carbonation samples are presented in Fig. 7; pressure- and temperature-dependent results of slurry carbonation samples can be found in Fig. S11 in the Supplementary Content. A total of ten different carbonate phases were detected, ranging from pure Ca-carbonates (namely calcite ($CaCO_3$), aragonite ($CaCO_3$), vaterite ($CaCO_3$) and monohydrocalcite ($CaCO_3 \cdot H_2O$)), to Ca-Mg-carbonates (magnesian calcite ($Ca_{1-0.85}Mg_{0-0.15}CO_3$), dolomite ($CaMg(CO_3)_2$) and huntite ($Mg_3Ca(CO_3)_4$)), to pure Mg-carbonates (magnesite ($MgCO_3$), nesquehonite ($MgCO_3 \cdot 3H_2O$) and hydromagnesite ($Mg_5(CO_3)_4(OH)_2 \cdot 4H_2O$)).

Calcium-containing carbonates were the predominant products after carbonation, given the high calcium content of the slags. Calcite is generally the most common mineral variety, followed by aragonite and monohydrocalcite; no significant amount of vaterite was detected. Aragonite formation predominates in slurry carbonated samples, especially those treated to

higher temperatures (see Fig. S11); its formation is known to be promoted under elevated temperatures (≥ 70 °C) and in the presence of Mg-ions (Santos et al., 2012a). Conversely, monohydrocalcite was observed almost exclusively in thin-film carbonated samples, where the milder process conditions, higher reaction pH and/or slower reaction kinetics may aid in its stability. Nishiyama et al. (2013) found a positive correlation between higher reacting solution pH and preferential formation of monohydrocalcite over anhydrous $CaCO_3$. In fact, the basicity of CC slag is higher than that of AOD slag (more details in Section 3.3), which may explain the greater monohydrocalcite content found in thin-film carbonated CC slags (Fig. 7a). In addition, Fukushi et al. (2011) have shown that monohydrocalcite is an intermediate product in the transition of amorphous calcium carbonate to stable calcite or aragonite. This may explain its time-dependent behavior, as it appears to form after prolonged periods (≥ 26 h) in the CO_2 chamber.

Substantial amounts of Ca-Mg-carbonates also form, especially magnesian calcite, followed by the more Mg-rich dolomite. Furthermore, their presence seems to occur in samples that contain less calcite and aragonite. This suggests that under certain conditions the Mg-ions that inhibit calcite growth and promote aragonite formation become trapped in the forming crystal, and as the Mg substitution in the $CaCO_3$ matrix creates strains on the crystalline structure that increase its solubility (Railsback, 2006), mineralogy evolution towards magnesian calcite takes place. Carbonated slag samples that contain more magnesian calcite also tend to contain greater quantities of other Mg-containing carbonates, although there is no clear trend with regards to time, temperature or pressure dependency. Nesquehonite and hydromagnesite are the predominant Mg-carbonates formed, both in thin-film and slurry carbonation. However, nesquehonite is more commonly found in AOD slag samples, while hydromagnesite is almost exclusively seen in CC slag samples. Zhang et al. (2006) suggest that hydromagnesite is preferentially formed over nesquehonite at higher pH; the higher basicity of CC slag compared to AOD slag (discussed in Section 3.3) may explain this difference in Mg-carbonate mineralogy. Huntite and magnesite, though detected, are usually quantified under the margin of error attributed to each sample based on QXRD uncertainty (plotted on each figure). The preferential formation of hydrated Mg–carbonates over the anhydrous magnesite is explained by the large ionic potential of Mg, which promotes hydration in solution (Railsback, 2006).

3.3 Heavy metal leaching

DOI:10.1016/j.ijggc.2013.04.004

Mineral carbonation of stainless steel slags not only serves to capture CO_2, but is also beneficial to improving geochemical properties of the material, thus helping to meet safe disposal or re-utilization requirements (Baciocchi et al., 2010; Huijgen and Comans, 2006; Santos et al., 2012c). Leaching tests were used to observe the effect of carbonation on the basicity of the solid samples, expressed by pH value in water, and on the heavy metals leached from these solids into solution. Carbonation can have an effect on these parameters due to three phenomena. Firstly, calcium and magnesium hydroxides, originating from the hydration of free oxides or silicates, convert to carbonates. The pH value of pure $Ca(OH)_2$ in solution is 12.4 at 25^{o}C (predicted by geochemical modelling); likewise the pH of $CaCO_3$ in solution is 8.2–9.9 (depending on CO_2 saturation in solution). As a result, it is expected that fully carbonated slags exhibit lower basicity. Secondly, the formation of a carbonate layer blocks access of inner unreacted alkaline minerals to the solution. This can also contribute to a gradual pH reduction as a function of carbonation progression (Santos et al., 2012b). Lastly, the conversion of some metal (hydr)oxides to metal carbonates changes the solubility of these metals (e.g. $BaCO_3$, $PbCO_3$, $ZnCO_3$ (Fernández-Bertos et al., 2004)).

Fig. 8 confirms the aforementioned hypotheses. Data of slurry carbonation are plotted together for samples carbonated for different times, temperatures and CO_2 partial pressures to illustrate the trend as a function of CO_2 uptake. Thin-film carbonation data correspond to samples collected at varying treatment times. Samples with greater CO_2 uptake, and thus higher carbonation conversion, exhibited lower pH. Particularly, the greater reaction extents obtained by slurry carbonation resulted in better basicity improvement compared to thin-film carbonation. It was possible to reduce the pH of AOD/CC slags from11.7/12.3 to as low as 9.4/9.7 after slurry carbonation, compared to 10.9/10.8 for the longest duration of thin-film carbonation. Compared to our previous study (Santos et al., 2012b), performed under atmospheric pressure bubbling slurry conditions and yielding maximal basicity reductions to pH of 9.9/10.1, the pH values from pressurized slurry carbonation have been improved due to greater carbonation conversions, entering the range of $CaCO_3$ basicity control. Basicity reduction as a function of CO_2 uptake progresses approximately linearly. It is likely that pH is initially controlled by silicate hydrates (above pH 11 (Chen et al., 2004)), followed by hydrated carbonates (below pH 10.8, assessed by geochemical modelling), and finally by $CaCO_3$ polymorphs below pH 10. It is also notable that AOD slag basicity is lower than that of CC slag initially, and remains so for comparable levels of CO_2 uptake. This may be due to, other than mineralogical differences, greater exposure of the slag's different alkaline minerals (which have different solubilities and reactivities towards hydration and carbonation) to the

aqueous medium, given the observed differences in particle morphology (Fig. 4 and Fig. S7). As carbonate precipitation is accelerated at high pH, the differing slag basicities, potentially buffering the carbonating medium to slightly different pH levels, could play a role in the greater CO_2 uptakes achieved by CC slag at comparable pH values (as inferred on Fig. 8).

The heavy metal leaching values of the solutions for which pH was measured are presented in Fig. 9 for slurry carbonation, and in Fig. S12 in the Supplementary Content for thin-film carbonation. The heavy metals measured correspond to those presented in Table 3, eleven of which are currently regulated in Wallonia (Belgium) for materials re-use. The concentrations of As in all solutions were below the detection limit of ICP-MS, and are therefore not reported. Horizontal dashed lines in the figures indicate the regulatory limits of respective elements; where no line is seen, the limit is greater than all measured values and the plotted y-axis scale. Accordingly, only four elements present significant leaching risk: Cr, Mo, Pb and Zn.

The rightmost data point of each data series on the graphs, at the highest pH, corresponds to the fresh slag; all other points are carbonated samples. Fresh AOD slag does not exceed any limit, though it comes close for Cr and Zn. Fresh CC slag exceeds limits for Cr and Pb, and approaches those for Mo and Zn. Carbonation successfully decreases leaching of Mo, Pb and Zn, where slurry carbonated samples (Fig. 9) generally fall farther below leaching limits than thin-film carbonated samples (Fig. S12). Results for Pb and Zn meet the expectations based on the review of Fernández-Bertos et al. (2004). It was reported in Santos et al. (2012c) that Mo leaching increased slightly after direct hot-stage carbonation of BOF slag. Cornelis et al. (2008) suggests that Mo leaching can slightly increase, remain constant or decrease as the pH lowers, depending on the speciation of Mo. Decreased Mo leaching is attributed in that study to the formation of $PbMoO_4$. As CC slag contains more Pb than AOD and BOF slags, it is possible that this mechanism explains the observed behavior from slurry carbonated samples.

In the case of Cr, the heavy metal present by far in greatest quantities in the slags (Table 1), some samples fall or remain under the limit while others remain or go above (leaching from fresh CC slag being higher than from AOD slag). Nevertheless, there appears to be some convergence to low leaching values once the sample pH reaches ~10 or lower; accordingly, this only occurs for the better carbonated slurry samples. The variability in Cr leaching could have its roots in the array of uptake mechanisms described by Fernández-Bertos et al. (2004). They report the possibility of Cr associating with calcium silicate hydrate (CSH) as a silicon substitute at higher pH values; but this mineral phase can undergo

solubilisation at lower pH, re-releasing Cr. At lower pH values still, calcite and neoformed double metal salts can take up Cr and again reduce leaching. Cornelis et al. (2008) geochemically modelled several Cr-containing species that may be responsible for its pH-dependent behavior, the three of which most likely participate being: $Ca_2Cr_2O_5 \cdot 6H_2O$ (i.e. substituted CSH), $Cr(OH)_3$, and $PbCrO_4$. While carbonation-induced reduction of Cr leaching appears to be mild, if not debatable, Van Gerven et al. (2005) showed that Cr-containing untreated bottom ashes brought to the same lower pH as carbonated ashes, by acidification, show much higher Cr leaching, meaning that Cr speciation in carbonated samples at least offers a buffer that hinders drastic solubilisation.

It is also possible to make some useful observations from the leaching results of the nine remaining heavy metals that do not pose a threat to exceeding regulatory limits. Positive correlations of leaching reduction with carbonation extent can be made for Ba, Cd, Co*, Cu, Ni*, Sb* and Se. The starred elements correspond to those for which improvement was substantial only in slurry carbonation. Leaching of Ti was generally low compared to the regulatory limit, even for the higher outliers. Leaching of V increased by roughly one order of magnitude compared to fresh sample values, with greater increase observed from thin-film carbonated samples (Fig. S12). Leaching of V is not currently regulated, but if its future leaching value is similar to those of other currently regulated metalloids (i.e. 1–2 mg/kg), its leaching could become a concern. Still, the risk of V leaching from stainless steel slags appears to be milder than from BOF slag, where carbonation induced solubilisation can reach upwards of 10 mg/kg (Santos et al., 2012c).

It should also be noted that aqueous carbonation forms the encapsulating carbonate layer previously presented (Fig. 4) that is not observed in direct hot-stage carbonation. This passivating layer, though detrimental for carbonation reaction progression, may play an important role in limiting heavy metal leaching by reducing exposure of the unreacted or unreactive phases in the particle core to the aqueous medium. The good homogeneity of slurry carbonation may explain beyond its better CO_2 uptake the reason for its generally superior leaching performance compared to thin-film carbonation. This can be particularly ascribed to the V leaching behavior from thin-film carbonated slag (Fig. S12), where the lower pH of the overall sample may exacerbate V leaching from some less carbonated particles.

4. Discussion

The slags herein tested (freshly produced AOD slag in absence of boron additives and as produced CC slag) proved ideal for mineral carbonation as their powdery morphology forgoes the need for costly milling (required for EAF and BOF carbonation) and provides sufficient surface area to impart high reactivity towards direct aqueous carbonation. The stainless steel slags were also verified to capture more CO_2 than BOF slag as reported by Huijgen et al. (2005) and EAF slag as reported by Baciocchi et al. (2011); it was possible to reach 21–24 wt%,CO_2 with AOD and CC slags compared to a maximum ~15 wt%,CO_2 with finely milled BOF and EAF slags.

It was also made apparent that high temperatures and pressures are not required for extensive carbonation of AOD and CC slags, which can have a positive impact on processing costs recently reported in literature. Kelly et al. (2011) assumed 35.5 bar, 200 ^{o}C, and no heat recovery, to model a carbonation process based on the data of Huijgen et al. (2005), and concluded that the energy penalty is too high. On the contrary, slurry carbonation makes it possible to harvest the exothermic heat generated by the carbonation reaction (Santos et al., 2013), and present results show that 90 °C and 9 bar,CO_2 suffice for rapid reaction. Even milder conditions can be used to further reduce processing costs, if necessary, with small loss of CO_2 uptake if well optimized.

Mineral carbonation conversion was accompanied by significant reduction in basicity, as much as two pH units after slurry carbonation. The stabilization of heavy metals leaching was also assessed. It was shown that these slags do not pose significant leaching risks compared to Belgian (Wallonia) regulatory limits for waste materials re-use, and that carbonation serves to further reduce the leaching of most heavy metals, in particular slurry carbonation. The only metal that approached limiting values was Cr, which is present in significant quantities in the slags and thus warrants observation as to its behavior, although several carbonated samples remained below the limit. Durinck et al. (2008) reviewed several methods by which Cr can be better stabilized through alterations to the hot-stage molten slag and its cooling trajectory. The recovery of Cr, a valuable metal, from stainless steel slags could also circumvent this issue, and is being investigated (Adamczyk et al., 2010).

Slurry carbonation was found to deliver greater mineral carbonation conversion and optimal treatment homogeneity, which are required to achieve high levels of CO_2 uptake, basicity reduction and heavy metal stabilization. However, these features are only required when the carbonated product is to be valorized beyond a carbon sink, for example as soil conditioner (pH control), as fine aggregate (sand substitute) in construction materials (e.g. concrete) or as mineral filler in chemical products (e.g. paints). In this manner, valorization

applications can potentially afford the additional processing costs associated with slurry carbonation. However, as Zingaretti et al. (2013) correctly suggest, thin-film carbonation may be a more feasible route for the utilization of slags as carbon sinks, particularly due to the elimination of CO_2 separation and compression and of liquid-solid separation, and in the reduction of heating and mixing demands. Prolonged treatment times (herein reported as long as 7 days under stationary conditions with intermittent de-agglomeration and re-wetting) may be reduced if the carbonating paste is more often de-agglomerated (to counter cementitious behavior) and re-wetted (to maintain required moisture content), for example with the application of a rotary drum as proposed by Zingaretti et al. (2013). In addition, the aforementioned valorization options envision direct use of the carbonated slags in commercial applications; however industrial symbiosis (Brent et al., 2012) and inter-industry solid residue utilization as blended materials (Mäkelä et al., 2012) should also be explored, as they can open new valorization routes, enable better energy/exergy efficiencies, and potentially diminish material property requirements commonly associated with commercial industrial reagents and products.

The present study also elucidated the mineralogical response of the stainless steel slags towards mineral carbonation by applying Rietveld refinement for the quantification of the mineral phases in the fresh and carbonated samples. Although the quantification uncertainty of this technique for complex mineral samples such as slags does not allow for precise measurement of carbonation kinetics, it was possible to qualitatively differentiate mineral phases that react more substantially than others over time, to observe noticeable differences in reactivity at varying process conditions (T and P), and to discern the preferential formation of certain Ca- and Mg-carbonates (mainly calcite, aragonite, magnesian calcite, monohydrocalcite, nesquehonite and hydromagnesite) depending on the processing route and operating conditions.

In a recent work of our research group, reported in Bodor et al. (2013), it was assessed if the carbonation conversion limitations could be attributable to differences in the susceptibility towards mineral carbonation of individual alkaline mineral phases present in steel and stainless steel slags. To this end, seven minerals were synthesized by solid-state sintering and carbonated individually. The results suggest that mineralogical susceptibility towards mineral carbonation is not the only determining factor controlling carbonation reactivity and CO_2 uptake. Particle morphology, in particular grain size and location of the mineral phase components, appears to be equally important, as reactive mineral phases dispersed within less reactive phases do not have the same opportunity to react with CO_2 as if

they were directly exposed to the reactive medium. Such distinctions may also affect basicity and pH buffering levels, which can potentially influence carbonation rate and conversion.

These points can be related to the fact that CC slag clearly carbonated more extensively than AOD slag at essentially every processing condition, despite the two slags having very similar chemical compositions and sharing essentially the same mineral phases, though in differing proportions. Unequal cooling trajectories during slag production may be responsible for controlling particle microstructure. In a way this is inopportune, as substantially more AOD slag is produced during steelmaking. On the other hand, it suggests that AOD mineralogy and particle morphology should be tuned to resemble more closely that of CC slag, either via additions to the hot-stage molten slag, or via precise control of the slag cooling path (i.e. the quenching rate). Durinck et al. (2008) describe this as 'slag engineering', by which the links between process parameters, slag microstructure and product properties are leveraged to turn secondary materials into tailored resources.

5. Conclusion

The metallurgical industry is in need of novel valorization routes to steer slags away from traditional storage in landfills and into valuable applications. At the same time, the technological field of mineral carbonation is in need of a process that is economical and scalable, to serve as a platform for its dissemination and uptake by several industrial activities that can benefit from it but are still skeptical of its merit. The results herein presented are promising for the valorization of carbonated AOD and CC stainless steel slags as secondary raw materials, or at least for the reduction of disposal costs and environmental impact of landfilled slags and their utilization solely as carbon sinks.

Acknowledgements

The KU Leuven Industrial Research Fund (IOF) is gratefully acknowledged for funding the Knowledge Platform on Sustainable Materialisation of Residues from Thermal Processes into Products (SMaRT-Pro²) in which this work was performed. R.M.S is thankful for financial support from the Natural Sciences and Engineering Research Council of Canada (NSERC) by a PGS-D scholarship. The KU Leuven Department of Metallurgy and Materials Engineering is acknowledged for the use of XRF and SEM-EDX equipment.

DOI:10.1016/j.ijggc.2013.04.004

Appendix A. Supplementary content

References

Adamczyk, B., Brenneis, R., Adam, C., Mudersbach, D., 2010. Recovery of Chromium from AOD-Converter Slags. Steel Research International 81, 1078–1083.

Baciocchi, R., Costa, G., Di Bartolomeo, E., Polettini, A., Pomi, R., 2010. Carbonation of Stainless Steel Slag as a Process for CO_2 Storage and Slag Valorization. Waste and Biomass Valorization 1, 467–477.

Baciocchi, R., Costa, G., Di Bartolomeo, E., Polettini, A., Pomi, R., 2011. Wet versus slurry carbonation of EAF steel slag. Greenhouse Gases: Science and Technology 1, 312–319.

Bodor, M., Santos, R.M., Kriskova, L., Elsen, J., Vlad, M., Van Gerven, T., 2013. Susceptibility of mineral phases of steel slags towards mineral carbonation: mineralogical, morphological and chemical assessment. European Journal of Mineralogy, in press.

Brent, G.F., Allen, D.J., Eichler, B.R., Petrie, J.G., Mann, J.P., Haynes, B.S., 2012. Mineral Carbonation as the Core of an Industrial Symbiosis for Energy-Intensive Minerals Conversion. Journal of Industrial Ecology 16, 94–104.

Chang, E.-E., Chen., C.-H., Chen, Y.-H., Pan, S.-Y., Chiang, P.-C., 2011a. Performance evaluation for carbonation of steel-making slags in a slurry reactor. Journal of Hazardous Materials 186, 558–564.

Chang, E.-E., Chiu, A.-C., Pan, S.-Y., Chen, Y.-H., Tan, C.-S., Chiang, P.-C., 2013. Carbonation of basic oxygen furnace slag with metalworking wastewater in a slurry reactor. International Journal of Greenhouse Gas Control 12, 382–389.

Chang, E.-E., Pan, S.-Y., Chen, Y.-H., Chu, H.-W., Wang, C.-F., Chiang, P.-C., 2011b. CO_2 sequestration by carbonation of steelmaking slags in an autoclave reactor. Journal of Hazardous Materials 195, 107–114.

Chang, E.-E., Pan, S.-Y., Chen, Y.-H., Tan, C.-S., Chiang, P.-C., 2012. Accelerated carbonation of steelmaking slags in a high-gravity rotating packed bed. Journal of Hazardous Materials 227– 228, 97–106.

Chen, J.J., Thomas, J.J., Taylor, H.F.W., Jennings, H.M., 2004. Solubility and structure of calcium silicate hydrate. Cement and Concrete Research 34, 1499–1519.

Cizer, Ö., Van Balen, K., Elsen, J., Van Gemert, D., 2012. Real-time investigation of reaction rate and mineral phase modifications of lime carbonation. Construction and Building Materials 35, 741–751.

Cornelis, G., Johnson, A., Van Gerven, T., Vandecasteele, C., 2008. Leaching mechanisms of oxyanionic metalloid and metal species in alkaline solid wastes: A review. Applied Geochemistry 23, 955–976.

Domínguez, M.I., Romero-Sarria, F., Centeno, M.A., Odriozola, J.A., 2010. Physicochemical Characterization and Use of Wastes from Stainless Steel Mill. Environmental Progress & Sustainable Energy 29, 471–480.

Doucet, F.J., 2010. Effective CO_2-specific sequestration capacity of steel slags and variability in their leaching behaviour in view of industrial mineral carbonation. Minerals Engineering 23, 262–269.

Durinck, D., Engström, F., Arnout, S., Heulens, J., Jones, P.T., Björkman, B., Blanpain, B., Wollants, P., 2008. Hot stage processing of metallurgical slags. Resources, Conservation and Recycling 52, 1121–1131.

Fernández-Bertos, M., Simons, S.J.R., Hills, C.D., Carey, P.J., 2004. A review of accelerated carbonation technology in the treatment of cement-based materials and sequestration of CO_2. Journal of Hazardous Materials B112, 193–205.

Fukushi, K., Munemoto, T., Sakai, M., Yagi, S., 2011. Monohydrocalcite: a promising remediation material for hazardous anions. Science and Technology of Advanced Materials 12, 064702.

Hollingbery, L.A., Hull, T.R. 2012. The thermal decomposition of natural mixtures of huntite and hydromagnesite. Thermochimica Acta 528, 45– 52.

Huijgen, W.J.J., Comans, R.N.J., 2006. Carbonation of Steel Slag for CO_2 Sequestration: Leaching of Products and Reaction Mechanisms. Environmental Science & Technology 40, 2790–2796.

Huijgen, W.J.J., Witkamp, G.-J., Comans, R.N.J., 2005. Mineral CO_2 Sequestration by Steel Slag Carbonation. Environmental Science & Technology 39, 9676–9682.

Kelly, K.E., Silcox, G.D., Sarofim, A.F., Pershing, D.W., 2011. An evaluation of ex situ, industrial-scale, aqueous CO_2 mineralization. International Journal of Greenhouse Gas Control 5, 1587–1595.

Kriskova, L., Pontikes, Y., Cizer, Ö, Mertens, G., Veulemans, W., Geysen, D., Jones, P.T., Vandewalle L., Van Balen K., Bart Blanpain, B., 2012. Effect of mechanical activation

on the hydraulic properties of stainless steel slags. Cement and Concrete Research 42, 778–788.

Lackner, K.S., Butt, D.P., Wendt, C.H., 1997. Progress on binding CO_2 in mineral substrates. Energy Conversion and Management 38, S259–S264.

Mahieux, P.-Y., Aubert, J.-E., Cyr, M., Coutand, M., Husson, B., 2010. Quantitative mineralogical composition of complex mineral wastes – Contribution of the Rietveld method. Waste Management 30, 378–388.

Mäkelä, M., Harju-Oksanen, M.-L., Watkins, G., Ekroos, A., Dahl, O., 2012. Feasibility assessment of inter-industry solid residue utilization for soil amendment—Trace element availability and legislative issues. Resources, Conservation and Recycling 67, 1–8.

Mayes, W.M., Younger, P.L., Aumônier, J., 2008. Hydrogeochemistry of Alkaline Steel Slag Leachates in the UK. Water, Air & Soil Pollution 195, 35–50.

Ministère de la Région Wallonne, 2001. Arrêté du Gouvernement wallon favorisant la valorisation de certains déchets. Moniteur Belge 2, 23859–23883.

Nishiyama, R., Munemoto, T., Fukushi, K., 2013. Formation condition of monohydrocalcite from $CaCl_2$–$MgCl_2$–Na_2CO_3 solutions. Geochimica et Cosmochimica Acta 100, 217–231.

Railsback, L.B., 2006. Some Fundamentals of Mineralogy and Geochemistry. http://www.gly.uga.edu/railsback/FundamentalsIndex.html (Retrieved 15.12.2012).

Rosenqvist, J., Kilpatrick, A.D., Yardley, B.W.D., 2012. Solubility of carbon dioxide in aqueous fluids and mineral suspensions at 294 K and subcritical pressures. Applied Geochemistry 27, 1610–1614.

Santos R., François D., Vandevelde, E., Mertens, G., Elsen J., Van Gerven, T., 2010. Process intensification routes for mineral carbonation. Proceedings of the Third International Conference on Accelerated Carbonation for Environmental and Materials Engineering, (ACEME10), November 29–December 1, 2010, Turku, pp. 13–22.

Santos, R.M., Ceulemans, P., Van Gerven, T., 2012a. Synthesis of pure aragonite by sonochemical mineral carbonation. Chemical Engineering Research and Design 90, 715–725.

Santos, R.M., François, D., Mertens, G., Elsen, J., Van Gerven, T., 2012b. Ultrasound-intensified mineral carbonation. Applied Thermal Engineering, doi: 10.1016/j.applthermaleng.2012.03.035.

Santos, R.M., Ling, D., Sarvaramini, A., Guo, M., Elsen, J., Larachi, F., Beaudoin, G., Blanpain, B., Van Gerven, T., 2012c. Stabilization of basic oxygen furnace slag by hot-stage carbonation treatment. Chemical Engineering Journal 203, 239–250.

Santos, R.M., Van Gerven, T., 2011. Process intensification routes for mineral carbonation. Greenhouse Gases: Science and Technology 1, 287–293.

Santos, R.M., Verbeeck, W., Knops, P., Rijnsburger, K., Pontikes, Y., Van Gerven, T., 2013. Integrated mineral carbonation reactor technology for sustainable carbon dioxide sequestration: 'CO_2 Energy Reactor'. Energy Procedia (in press).

Snellings, R., Machiels, L., Mertens, G., Elsen, J., 2010. Rietveld refinement strategy for quantitative phase analysis of partially amorphous zeolitized tuffaceous rocks. Geologica Belgica 13, 183–196.

Van Gerven, T., Van Keer, E., Arickx, S., Jaspers, M., Wauters, G., Vandecasteele, C. 2005. Carbonation of MSWI-bottom ash to decrease heavy metal leaching, in view of recycling. Waste Management 25, 291–300.

Vandevelde, E. 2010. Mineral Carbonation of Stainless Steel Slag. Master's Thesis, KU Leuven.

Zhang, Z., Zheng, Y., Ni, Y., Liu, Z., Chen, J., Liang, X., 2006. Temperature- and pH-Dependent Morphology and FT-IR Analysis of Magnesium Carbonate Hydrates. The Journal of Physical Chemistry B, 110, 12969–12973.

Zingaretti, D., Costa, G., Baciocchi, R., 2013. Assessment of the energy requirements for CO_2 storage by carbonation of industrial residues. Part 1: Definition of the process layout. Energy Procedia (in press).

DOI:10.1016/j.ijggc.2013.04.004

List of Figures

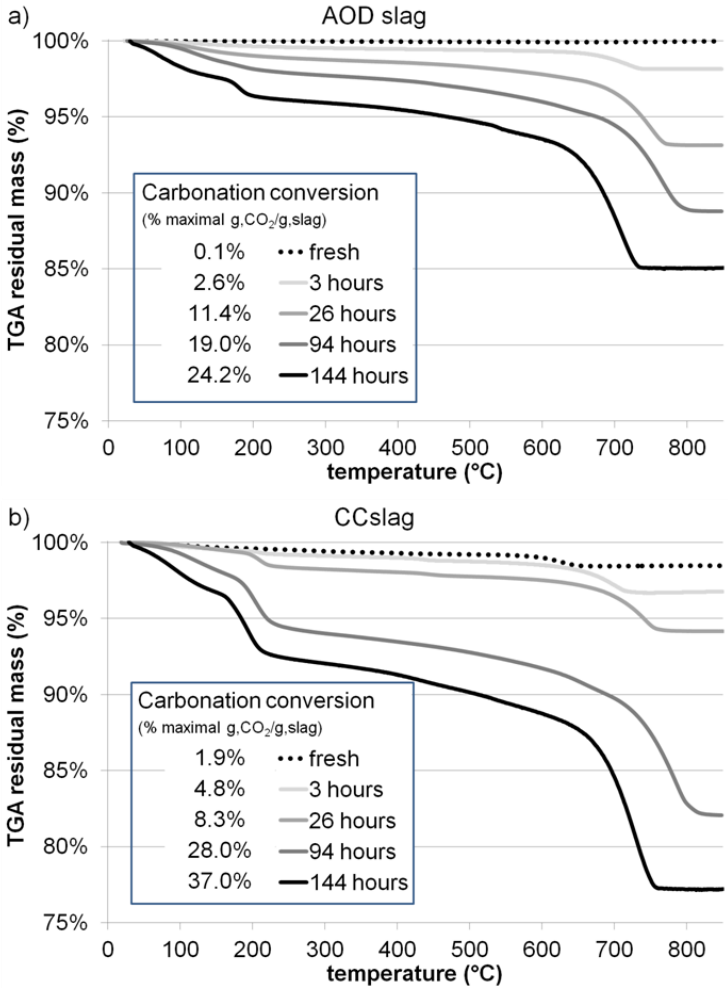

Fig. 1. Thin-film carbonation results: thermogravimetrical curves and carbonation conversion values for AOD (a) and CC (b) slags as a function of reaction time; $P(CO_2)$ = 0.2 atm, T = 30 °C, L/S = 25 wt%, 95% relative humidity.

DOI:10.1016/j.ijggc.2013.04.004

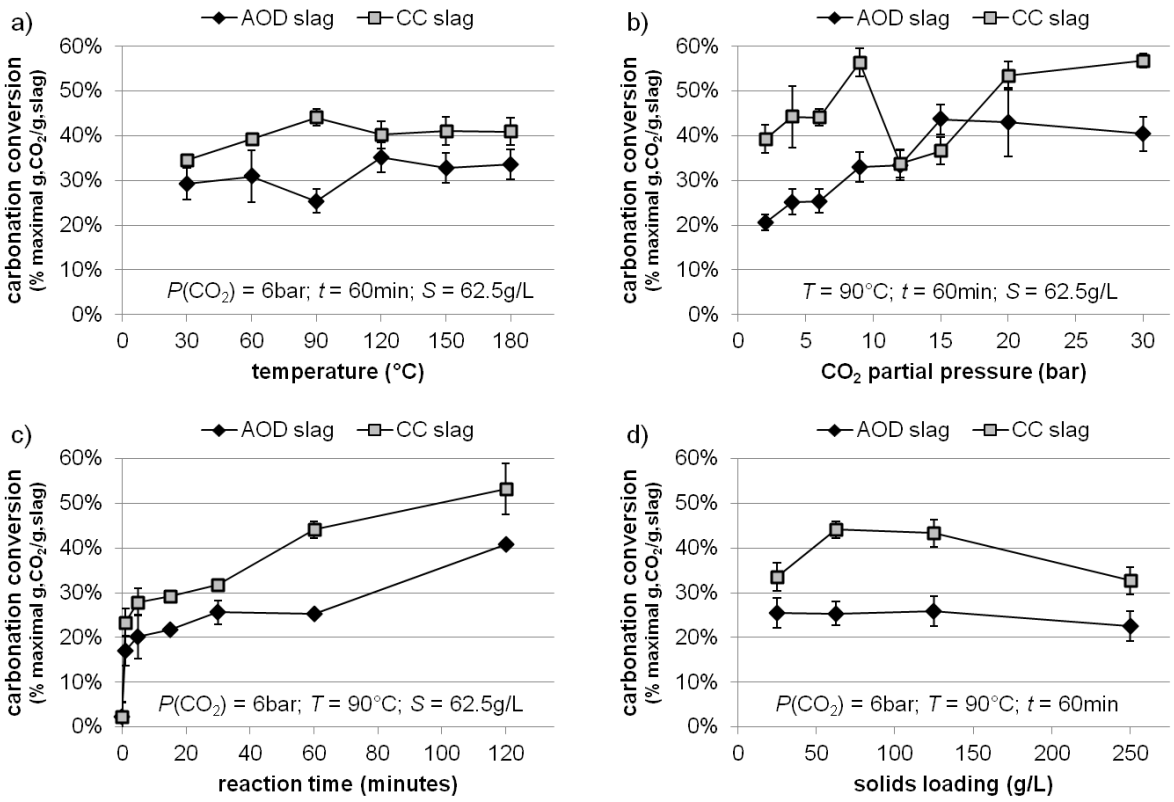

Fig. 2. Slurry carbonation results: effect of temperature (a), CO_2 partial pressure (b), reaction time (c) and solids loading (d) on the carbonation conversion of AOD and CC slags; error bars reflect reproducibility data presented in Fig. S6 in the Supplementary Content).

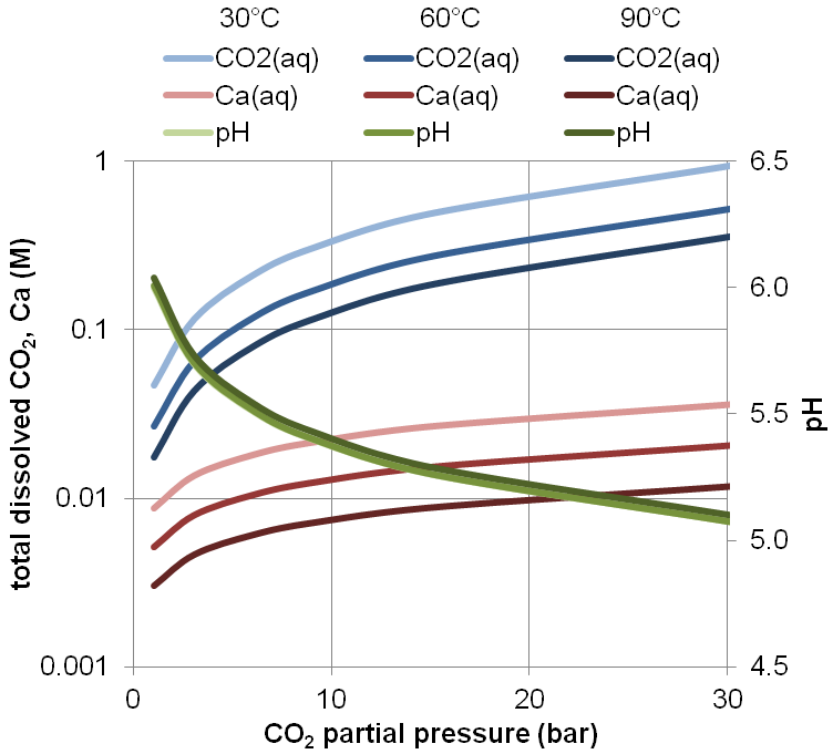

Fig. 3. Geochemical modeling of $CO_2/CaCO_3/H_2O$ equilibrium: effects of temperature and CO_2 partial pressure on total dissolved species and pH.

DOI:10.1016/j.ijggc.2013.04.004

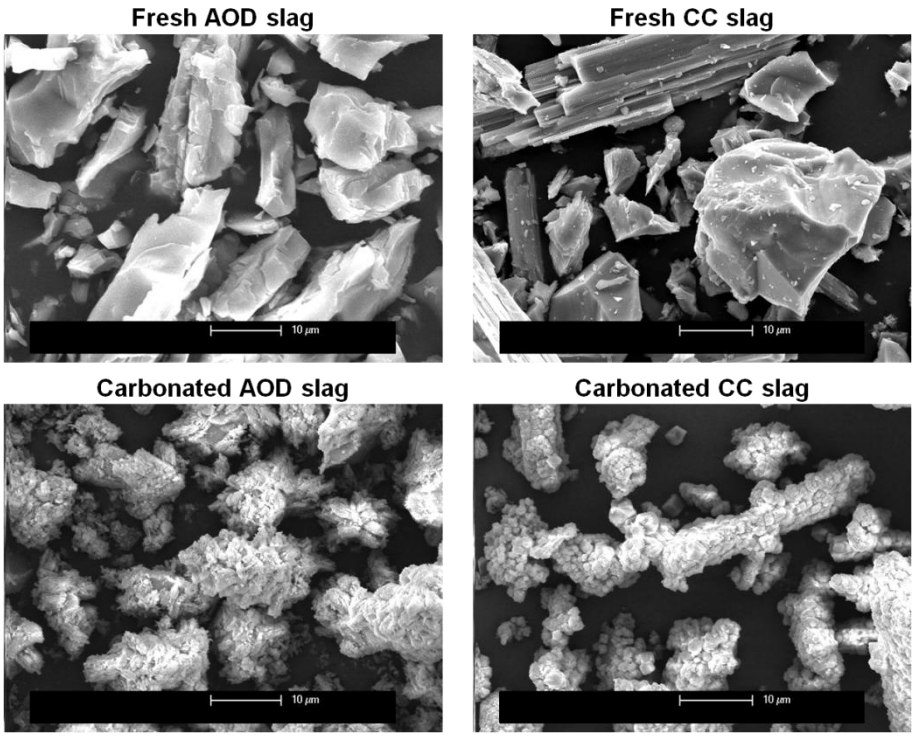

Fig. 4. Fresh and carbonated (120 minutes) slag particle morphology.

DOI:10.1016/j.ijggc.2013.04.004

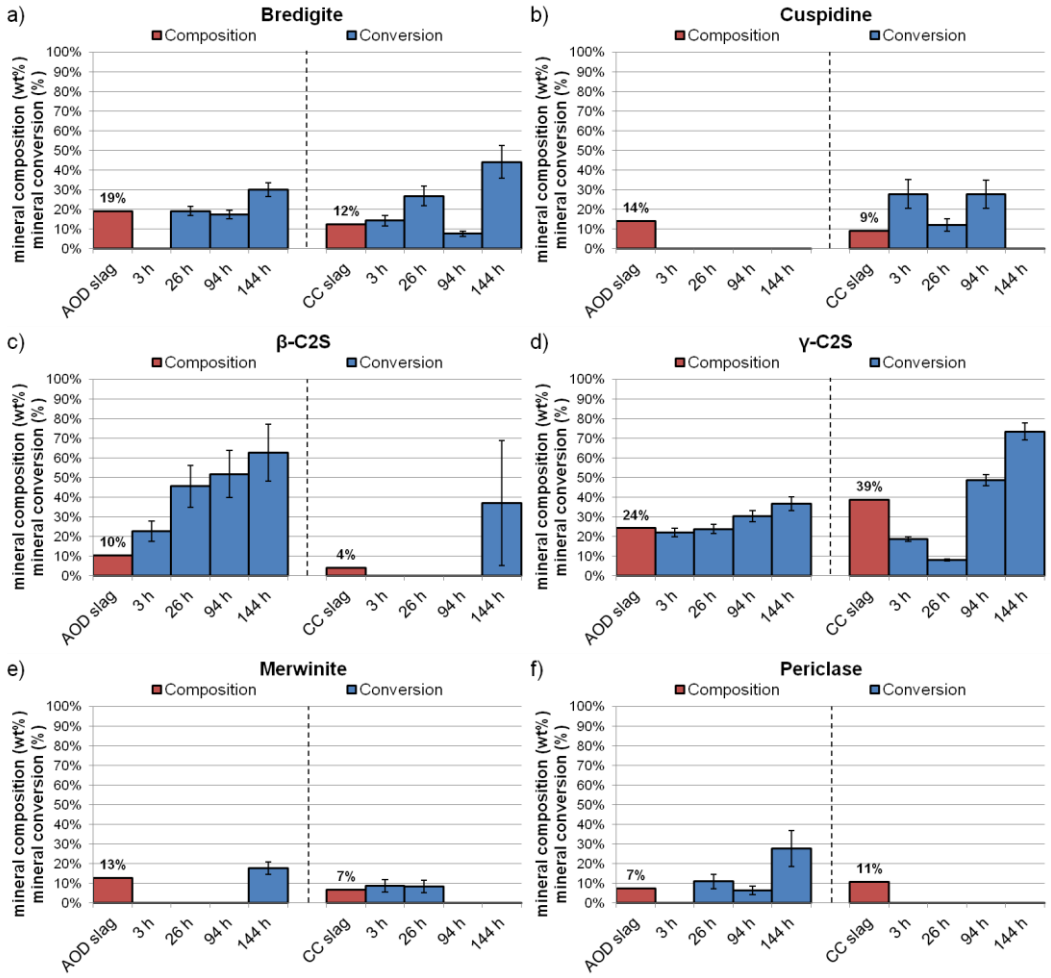

Fig. 5. Thin-film carbonation results: carbonation conversion of slag mineral phases (bredigite (a), cuspidine (b), β-C2S (c), γ-C2S (d), merwinite (e) and periclase (f)) as a function of reaction time; $P(CO_2)$ = 0.2 atm, T = 30 °C, L/S = 25 wt%, 95% relative humidity; error bars represent mean quantification accuracy, based on select replicate analyses, of ± 2.3 wt% of the quantified amount.

DOI:10.1016/j.ijggc.2013.04.004

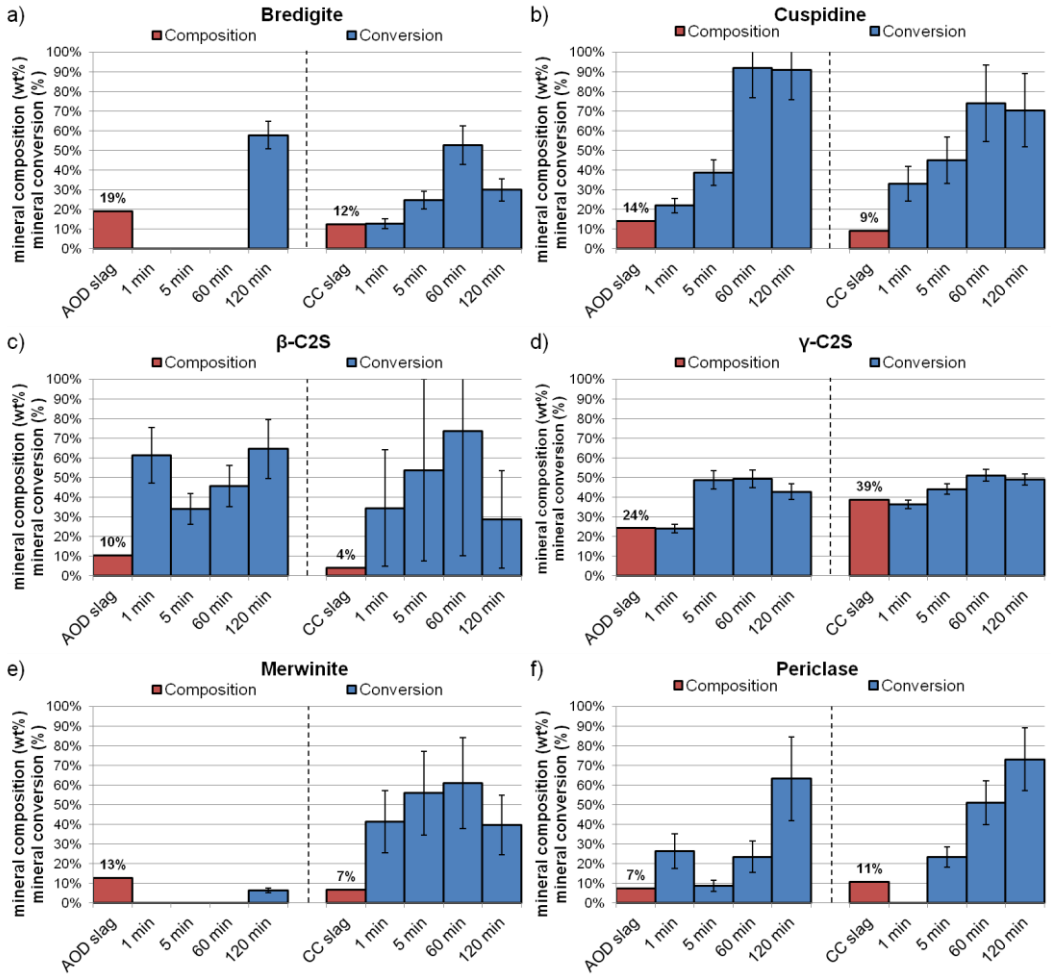

Fig. 6. Slurry carbonation results: carbonation conversion of slag mineral phases (bredigite (a), cuspidine (b), β-C2S (c), γ-C2S (d), merwinite (e) and periclase (f)) as a function of reaction time; $P(CO_2)$ = 6 bar, T = 90 °C, S = 62.5 g/L; error bars represent mean quantification accuracy, based on select replicate analyses, of ± 2.3 wt% of the quantified amount.

DOI:10.1016/j.ijggc.2013.04.004

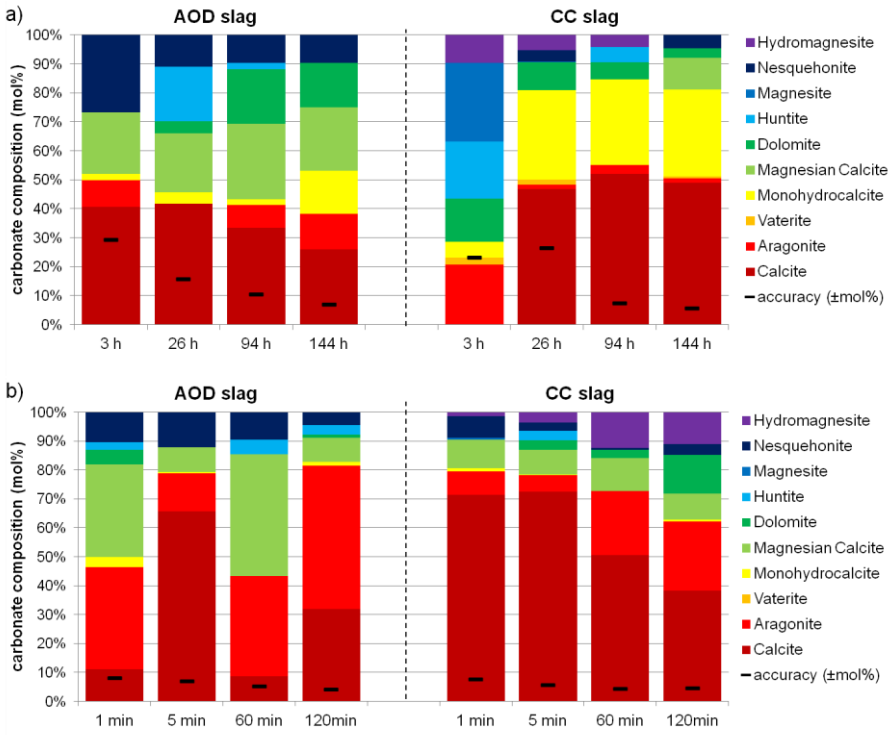

Fig. 7. Composition of carbonate mineral phases (normalized to 100 % of carbonate content) for thin-film carbonation (a) and slurry carbonation (b) as a function of reaction time; error bars represent mean quantification accuracy, based on select replicate analyses, of ± 2.3 wt% of the quantified amount.

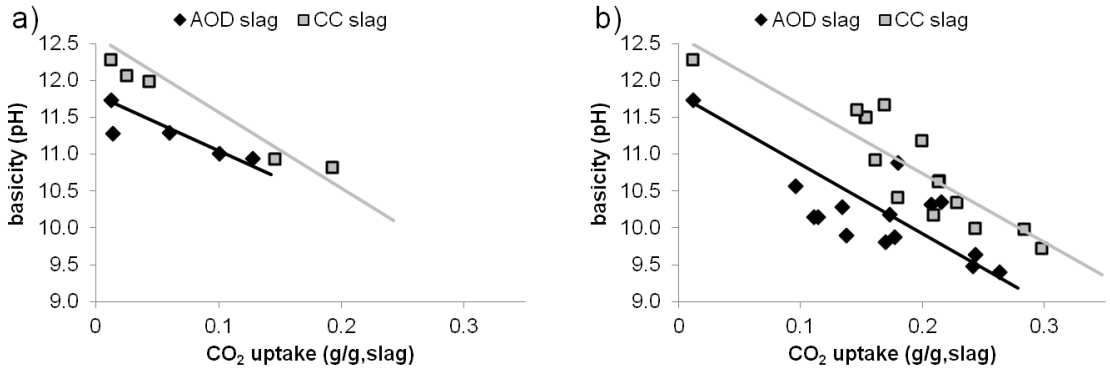

Fig. 8. Basicity of stainless steel slag samples from thin-film carbonation (a) and slurry carbonation (b) as a function of CO_2 uptake.

DOI:10.1016/j.ijggc.2013.04.004

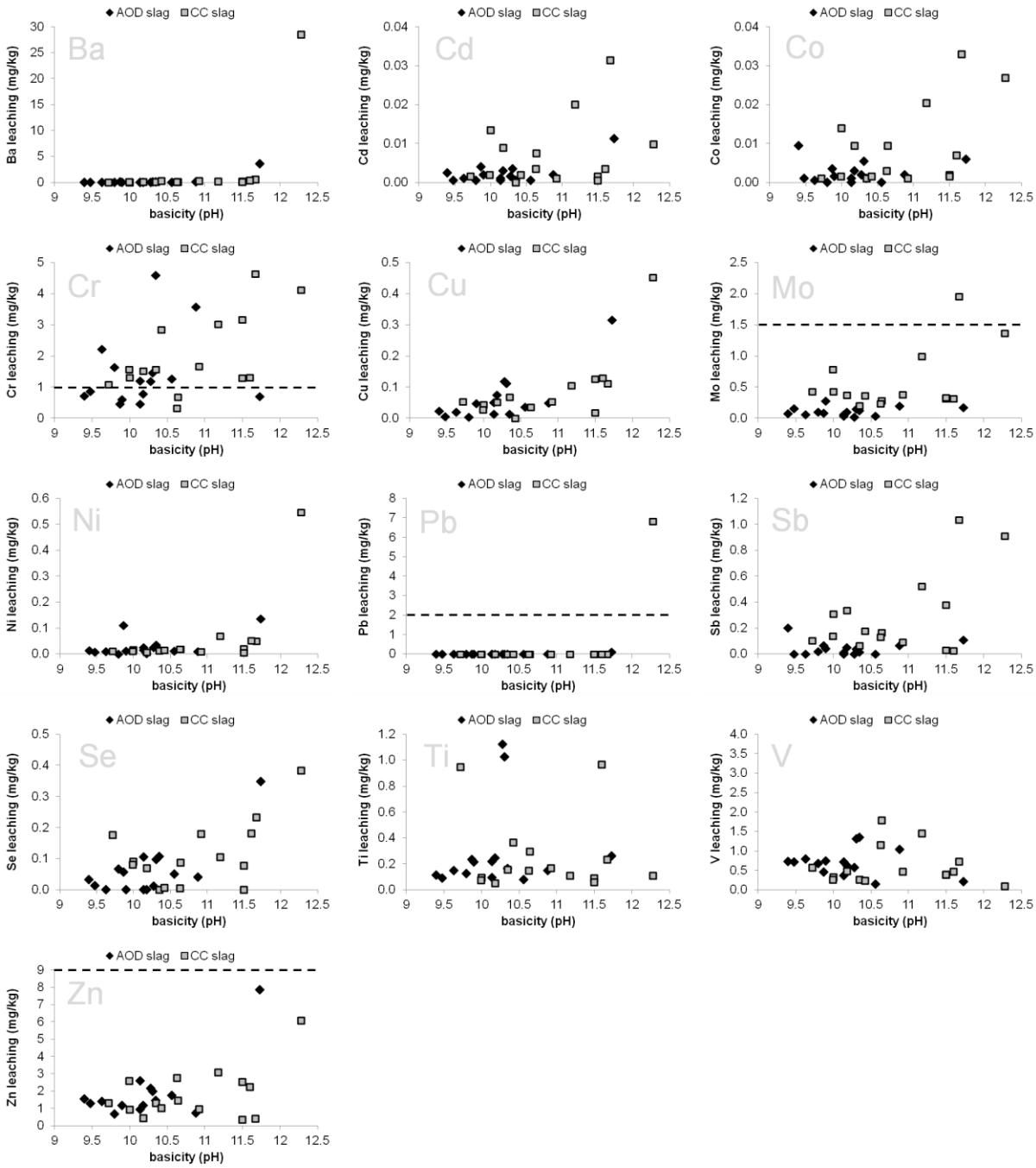

Fig. 9. Slurry carbonation results: leaching of heavy metals from stainless steel slags as a function of pH. Horizontal dashed lines indicate Belgian (Wallonia) regulatory limits; where no line is seen, the limit is greater than the y-axis shown.

DOI:10.1016/j.ijggc.2013.04.004

List of Tables

Table 1
Chemical composition of steel slags determined by XRF and expressed as elements (> 0.1 wt%) and oxides, and loss on ignition (LOI) determined by TGA.

Elements (wt%)	Al	Ca	Cr	Fe	Mg	Mn	S	Si	Ti	
AOD slag	0.74	39.2	0.52	0.17	5.4	0.32	0.24	15.2	0.24	
CC slag	0.57	35.8	3.4	1.1	6.6	0.39	0.25	12.8	0.51	
Oxides (wt%)	Al_2O_3	CaO	Cr_2O_3	Fe_2O_3	MgO	MnO	SO_3	SiO_2	TiO_2	LOI
AOD slag	1.4	54.8	0.76	0.25	9.0	0.42	0.24	32.5	0.40	0.10
CC slag	1.1	50.0	5.0	1.6	10.9	0.50	0.63	27.4	0.86	1.5

Table 2
Mineral composition (wt%) of stainless steel slags determined by QXRD with Rietveld refinement (three largest values bolded).

Mineral	Chemical formula	AOD slag wt%	CC slag wt%
Åkermanite	$Ca_2MgSi_2O_7$	3.3	1.8
Bredigite	$Ca_7Mg(SiO_4)_4$	**18.9**	**12.4**
Cuspidine	$Ca_4Si_2O_7F_2$	**13.9**	9.1
β-Dicalcium silicate	Ca_2SiO_4	10.2	3.9
γ-Dicalcium silicate	Ca_2SiO_4	**24.1**	**38.6**
Enstatite	$Mg_2Si_2O_6$	3.9	9.7
Fayalite	Fe_2SiO_4	0.8	1.9
Gehlenite	$Ca_2Al_2SiO_7$	1.1	0.2
Lime	CaO	0.1	0.6
Magnetite	Fe_3O_4	0.4	2.1
Merwinite	$Ca_3Mg(SiO_4)_2$	12.7	6.7
Periclase	MgO	7.4	**10.7**
Portlandite	$Ca(OH)_2$	0.4	1.4
Quartz	SiO_2	0.5	0.4
Wollastonite	$CaSiO_3$	2.4	0.4
Amorphous	-	nd	nd
Sum		100	100

nd = not detected, using internal standard (corundum) methodology of Snellings et al. (2010).

Table 3
Heavy metal leaching limits for waste material re-use in Belgium (Wallonia).

	As	Ba	Cd	Co	Cr[2]	Cu	Mo
Limit[1] (mg/kg)	1.0	N.R.	1.0	1.0	1.0	20	1.5
	Ni	Pb	Sb	Se	Ti	V	Zn
Limit[1] (mg/kg)	2.0	2.0	2.0	N.R.	20	N.R.	9.0

[1] Regulation: DIN 38414/EN 12457-4/CEN TC 292 (Ministere De La Region Wallonne, 2001)
[2] Limits prescribed for Cr(VI), whereas total Cr measured.
N.R.: not regulated.

DOI:10.1016/j.ijggc.2013.04.004

Table 4
Thin-film carbonation results: sample moisture (wt%) as a function of reaction time.

	AOD slag wt%	CC slag wt%
Initial	25.0	25.0
3 hours	22.1	23.2
26 hours[1]	17.8	14.1
26 hours re-wetted	25.9	22.9
94 hours[2]	17.6	3.8
94 hours re-wetted	29.3	19.3
144 hours	19.3	6.7

[1] Subsequently re-wetted with additional 2/5 of initial moisture content.
[2] Subsequently re-wetted with additional 3/5 of initial moisture content.